



Extreme precipitation and flooding in Berlin under climate change and effects of selected grey and blue-green measures

Franziska Tügel^{1,3,4}, Katrin M. Nissen², Lennart Steffen¹, Yangwei Zhang¹, Uwe Ulbrich², and Reinhard Hinkelmann¹

Correspondence: Franziska Tügel (franziska.tuegel@utwente.nl)

Abstract. This paper aims to quantify potential changes in extreme precipitation under climate change scenarios in the city of Berlin, Germany, and their resulting impacts on urban flooding in a selected flood-prone area of the city. Furthermore, it investigates the effectiveness of the existing drainage system, infiltration from unsealed surfaces, and retention roofs during extreme rainfall events under both current and future climate conditions.

The effect of climate change on the statistical distribution of extreme precipitation in Berlin is assessed by analyzing a single-model set of climate scenario simulations at convection permitting resolution (COSMO-CLM). Three 30-year periods are simulated: The historical period under observed greenhouse gas concentrations from 1971 to 2000 and two RCP8.5 scenario periods from 2031 to 2060 and from 2071 to 2100. For the historical period, the estimated 1-hour rainfall sum for a 100-year return level (referred to as 'Historical 100a') agrees well with the statistical values from station observations. For the period 2031-2060 under RCP8.5 conditions the respective rainfall sum of the 1-hour 100-year event (referred to as 'Future 100a') increases by 46% and the strongest hourly intensity in all three simulated 30-year periods (referred to as 'Strongest') is increased by 123% compared to the Historical 100a event.

The impacts of these increases in extreme precipitation on flooding characteristics in a Central-Berlin region around the Gleimtunnel, which is known for frequent pluvial flooding, are studied by conducting simulations with the 2D surface flow model hms⁺⁺ coupled to a 1D drainage model. The Future 100a event result in a 51% increase in the simulated maximum water depth, a 43% increase in maximum surface runoff at the local flooding hotspot Gleimtunnel, and a 33% increase in the volume of combined sewer overflow. For the Strongest event, the respective increases are 137% (maximum water depth), 296% (maximum surface runoff), and 74% (combined sewer overflow).

The effects of the existing drainage system and infiltration under different rainfall scenarios are highlighted by comparing simulation results with and without their consideration. Neglecting the drainage system results in a 170% increase for the Historical 100a event and a 110% increase for the Strongest event, compared to the reference simulations. While the drainage system strongly reduces flooding, especially at hotspots, it cannot fully prevent severe flooding, and its effectiveness decreases

¹Chair of Water Resources Management and Modeling of Hydrosystems, Technische Universität Berlin, Berlin, Germany

²Institute for Meteorology, Freie Universität Berlin, Berlin, Germany
³Department of Water Resources, Faculty of Geo-Information Science and Earth Observation (ITC), University of Twente, Enschede, The Netherlands

⁴Multidisciplinary Water Management, Civil Engineering and Management, Faculty of Engineering Technology, University of Twente, Enschede, The Netherlands





with higher rainfall intensity. Studying infiltration reflects potential impacts of surface sealing or, conversely, desealing as a climate adaptation strategy. Neglecting infiltration increases the maximum water depth at the Gleimtunnel by 33% for the Historical 100a event and 18% for the Strongest event compared to reference simulations. Infiltration significantly reduces flooding, though its effectiveness decreases with higher rainfall intensity.

As a potential adaptation strategy, the impact of replacing all roofs with retention roofs is examined. For this best-case adaptation scenario, the maximum water depth at the local hotspot is reduced by 22-24%, and the volume of combined sewer overflow by 15-20% in the different scenarios. Since full retention on all roof surfaces is considered for all rainfall scenarios, the effects are almost the same. Remarkably, the retention roofs significantly reduced the maximum surface runoff in the Gleimtunnel during the Strongest event to below the stability threshold for pedestrians, which was clearly exceeded in the simulation without retention roofs.

The results of this study highlight the potential local impacts of ongoing global warming in terms of heavy rainfall and urban flooding in the city of Berlin and emphasize the need to combine grey infrastructure, retention roofs, and other blue-green measures.

1 Introduction

While there is a European-wide obligation to produce risk maps for river floods (EUR-Lex, 2007), this is not the case for pluvial flooding. Nevertheless, such maps are being produced for more and more cities, including Berlin (Umweltatlas Berlin). Information maps for hotspots of heavy precipitation impact already exist for the whole city. These show ground depressions and fire brigade operations required in the past because of flooding. More detailed risk maps for pluvial flooding are currently only publicly available for 3 smaller areas within the city. These maps show the spatial extent of flooding, the flood depths and the flow velocities for three different heavy rainfall scenarios and are generated with coupled 2D-1D hydrodynamic models. The Federal Agency for Cartography and Geodesy (BKG) is currently working with the federal states to develop Germany-wide risk maps for pluvial flooding. The maps for northern and eastern Germany including Berlin should have become available until the end of 2023 (BKG, 2023). To the knowledge of the authors, this was not achieved until January 2025. The first subregion for the Germany-wide maps for pluvial flooding, North Rhine-Westphalia, has been available as an interactive web map since October 2021. The simulations are based on simplifications, such as no consideration of the underground drainage system and infiltration from permeable surfaces (BKG, 2021). These maps are based on hydrodynamic simulations using precipitation scenarios as input. These scenarios are categorized as rare, exceptional and extreme. The exceptional event is defined as a 100-year precipitation event (T = 100a) with a duration of one hour and an Euler type 2 (Euler-2) temporal evolution (e.g. Wartalska et al., 2020; DWA, 2006). For this purpose, statistical precipitation intensities from the coordinated heavy precipitation regionalization and evaluation (KOSTRA, 2020) of the German Weather Service (DWD) are used (see Sect. 2).

The problem with these statistical values is that they are based on historical observations and will be outdated soon according to climate simulations. Researchers agree in their assessment that over Central Europe extreme precipitation events will occur





more frequently and become more intense in a warmer climate (IPCC, 2022). To investigate possible future developments for a specific region, climate models that are driven by plausible greenhouse gas (GHG) scenarios can be analyzed. Ideally, for investigations focusing on extreme precipitation events, regional models with convection-permitting resolution are used for this task (e.g. Lucas-Picher et al., 2021). To determine extreme value statistics, long simulations are needed. These are computationally expensive and usually cover only small areas. At the time of writing only one suitable set of simulations at convection permitting resolution covering Berlin was available. We use these simulations to analyze possible changes in the statistical distribution of extreme precipitation in Berlin. The simulation set includes three 30-year periods under historical and Representative Concentration Pathway (RCP) 8.5 GHG conditions.

In the next step, the impacts of changes in extreme precipitation on the characteristics of pluvial flooding in a selected urban area are investigated using hydrodynamic model simulations. These simulations are conducted with the 2D shallow water model hms⁺⁺, which is bi-directionally coupled to the 1D Storm Water Management Model (SWMM). For example, Li et al. (2024) conducted similar investigations for an urban area in Haining, Zhejiang Province, China, using the SWMM model with the hydrological subcatchment approach, rather than coupling it with a 2D surface flow model. Neumann et al. (2024) carried out a detailed analysis of the effectiveness of different types of decentral nature-based solutions for flood reduction in another area of Berlin. While they also used a 2D/1D coupled modeling approach, roofs and measures were not represented as 2D surfaces, but through hydrological elements within SWMM. In our study, the focus is primarily on the effects of increased heavy precipitation on spatially distributed flood heights and surface runoff, temporal developments at a selected flooding hotspot, and combined sewer overflow. Furthermore, the effects of infiltration, the drainage system, and retention roofs as one example for blue-green infrastructure are studied. The following paragraphs briefly describe the basics of these processes and the motivation for studying their effects on urban flooding.

Infiltration is an important process in the water cycle. Rainfall intensities exceeding the infiltration capacity are generally considered as the reason for the formation of so-called Hortonian overland flow, which is often the type of overland flow during flash floods instead of saturated overland flow. In urban flood simulations, infiltration is sometimes neglected (e.g. Tügel et al., 2023), referring to the high degrees of surface sealing and choosing a conservative approach to "be on the safe side". But also in urban areas, understanding the effects of infiltration is crucial - for example, to estimate how further surface sealing could exacerbate flooding and to evaluate the potential flood reduction benefits of surface desealing.

The drainage system can be considered the most important grey infrastructure for mitigating surface flooding from rainfall. However, its dimensions are typically designed for return periods of only two to five years. In simulations of extreme rainfalls, the drainage system is sometimes neglected (Tügel et al., 2023) or considered with simplified approaches of reduced rainfall on sealed surfaces (Apel et al., 2024). In order to consider both the surface runoff and the flow in the drainage system, a bidirectionally coupled 2D-1D model is needed. To quantify the effectiveness of the drainage system on the reduction of surface flooding even for extreme precipitation events, this study compares simulation results with and without the consideration of the drainage system.

A coupled approach is also preferred as it allows the simulation of overflow events in cases where the drainage system is overstrained, which can exacerbate surface flooding at low-lying locations. In the case of a combined sewer system this leads





to severe pollution and hygienic problems in addition to flooding. In a combined sewer system rainwater and waste water share the same pipes, which is the case in the central districts of Berlin including the considered study area. While overflows from the drainage to the urban surface area usually only occur during very heavy events, combined sewer overflows of untreated mixed rain and sewage water into water bodies occur many times a year in Berlin causing severe environmental pollution. In this study we will also quantify the effect of different extreme precipitation scenarios on the combined sewer overflow.

In recent years to decades there is a paradigm shift from the aim of "transporting the rainwater as fast as possible out of the city" to "keeping as much rainwater as possible in the city". This should be achieved for example with blue-green infrastructure. The goal is to restore a more natural water balance in cities by decreasing surface runoff and flooding, increasing evapotranspiration and groundwater recharge and/or saving drinking water by using captured rainwater for non-potable water uses (Zevenbergen et al., 2018). Climate change is increasing the pressure on water resources, which makes this shift in the urban water management inevitable. Decoupling surfaces and holding back more rainwater inside the urban area should also relieve the drainage system itself and reduce the combined sewer overflows in case of heavy rain events. Blue-green infrastructure offers several benefits and can also help reduce urban flooding.

2 Data

100

110

105 2.1 Meteorological observations

KOSTRA-DWD (KOSTRA, 2020) is the official source for statistical extreme precipitation intensities in the time period 1951-2020. KOSTRA-DWD is compiled by the German Weather Service (DWD) on the basis of gridded precipitation observations. It lists the precipitation intensities of heavy rainfall events in terms of their duration and statistical return period. For the analysis, a duration dependent general extreme value distribution (d-GEV) is fitted to the annual maxima of the gridded observations (Junghänel et al., 2022; Koutsoyiannis et al., 1998). A key area of application is the dimensioning of stormwater management structures such as sewer networks, pumping stations, and retention basins, and they are also used to create flood maps for pluvial flooding. For comparisons with measurements at a local station, data from the weather station Berlin Dahlem is used.

2.2 Climate simulations

For this study precipitation for present day and climate change conditions is taken from simulations of the regional climate model COSMO-CLM at convection permitting resolution (CCLM-CPS). The simulations have been described in detail by Rybka et al. (2023). They are conducted at a horizontal resolution of 0.0275° (approx. 3 km). Deep convection is explicitly solved, while shallow convection is parameterized. Precipitation output is available at 1-hour aggregation period. The simulations cover Germany and surrounding regions in order to capture the the river basins that discharge towards Germany. The forcing data stems from the global climate model MIROC5 (Model for Interdisciplinary Research on Climate, Watanabe et al., 2011). CCLM-CPS simulations were conducted for 3 30-year periods: The historical period 1971 to 2000 and the RCP8.5 scenario periods 2031 to 2060 (near future) and 2071 to 2100 (far future) (Haller et al., 2022a, b). The ability of CCLM-CPS





to simulate extreme precipitation intensities has been analyzed by Rybka et al. (2023). It was found that CCLM-CPS for the historical period shows the best agreement with the KOSTRA estimate compared to several other regional model ensembles.

2.3 Ground properties

For the hydrodynamic simulations, the digital elevation model provided by Geoportal Berlin/ATKIS®DGM with 1 m spatial resolution was used, incorporating buildings based on Geoportal Berlin/ALKIS Gebäude. Land use types are based on the dataset Geoportal Berlin/ALKIS Berlin Tatsächliche Nutzung. Saturated hydraulic conductivity of the first 1 m of soil was taken from the dataset Umweltatlas Berlin/Bodenkundliche Kennwerte 2015. The sealing degree is taken from Umweltatlas Berlin/Versiegelung 2021. The aforementioned data from Geoportal Berlin and Umweltatlas Berlin are licensed under dl-de/by-2-0 (www.govdata.de/dl-de/by-2-0).

3 Methods

135

3.1 Return levels

Return levels are estimated using the method described by Fauer et al. (2021), which is an extension of the method used for KOSTRA-DWD. For each grid box located within the boundaries of Berlin, the annual maximum intensities (z) for different accumulation periods (durations d) are extracted from the climate simulations. The values for d=1 h are shown exemplary in Fig. 1. The probability distribution is modelled by fitting a duration dependent general extreme value distribution (d-GEV) to these maxima (Eq. 1). Five parameters need to be determined: The rescaled location parameter $\tilde{\mu}$, the scale offset σ_0 , the duration offset Θ , the duration exponent η , and the shape parameter ξ .

$$G(z) = exp\left\{ -\left[1 + \xi\left(\frac{z}{\sigma_0(d+\Theta)^{-\eta}}\right)\right]^{-1/\xi}\right\}. \tag{1}$$

For durations > 1 hour the resulting Intensity-Duration-Frequency (IDF) curves follow a power law, and the duration offset Θ , which describes the curvature, is negligible.

Our hypothesis is that the underlying distribution of the extreme precipitation at the horizontal resolution resolved by station observations and by the climate simulations does not exhibit spatial variations within Berlin and its immediate vicinity. We therefore assume that the spatial variations between neighboring grid boxes are a random effect caused by the limited number of observations (shortness of the time series). This is supported by the findings of Rybka et al. (2023) showing no indication for systematic patterns in observed extreme precipitation for both daily and hourly events in our study area. By pooling the data over all grid boxes located within the boundaries of Berlin we are able to include more data in the parameter estimation of the d-GEV distribution. This reduces the uncertainty associated with the parameter estimation and increases the robustness of the inferred climate change signal.





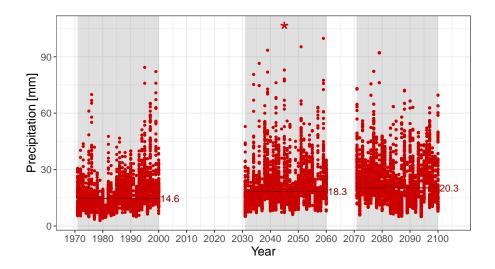


Figure 1. Annual maximum of hourly precipitation in CCLM-CPS simulation for all grid boxes in Berlin. Horizontal lines and corresponding labels denote the median over the simulation period. The Strongest event simulated is marked by an asterisk.

The fitting of the d-GEV distribution is conducted using the R-package IDF (Ulrich et al., 2020), which determines the parameters by minimizing the negative log-likelihood.

3.2 Hydrodynamic modeling

155

To investigate urban flooding generated by heavy rainfalls from climate simulations as well as effects of different mitigation measures, a 2D-1D hydrodynamic model is set up for one selected drainage catchment within the city of Berlin. The open-source 2D shallow water model hms⁺⁺ is used for the simulation of surface flow. It numerically solves the depth-averaged shallow water equations using a robust MUSCL scheme based on the finite volume method. Furthermore, the performance of the model has been optimized to achieve shorter computational times, and methods for further performance optimizations are currently under development. Details can be found in Simons (2020) and Steffen and Hinkelmann (2023). hms⁺⁺ is bidirectionally coupled to the 1D drainage model of the open-source Storm Water Management Model (SWMM) (Rossman and Huber, 2015). The surface model spans an area of approximately 13 km². It consists of 543 900 rectangular cells of 5 m cell length. A spatial resolution of 5 m was selected as a suitable compromise between computational time and accuracy of the numerical simulations. A finer resolution of 2 m was tested in a sensitivity study (see Sect. 4.3).

The drainage model was provided by the Berlin Water Company (BWB) consisting of overall 24 km pipe lengths including 1964 nodes and 2344 links. The system includes pumps, orifices, and weirs. The maximum depth of the conduits varies between 0.12 and 2 m. The Manning's friction coefficient of all conduits is 0.013 s/m^{1/3}, the entry loss coefficient 0.15 and the exit loss coefficient 0.015.

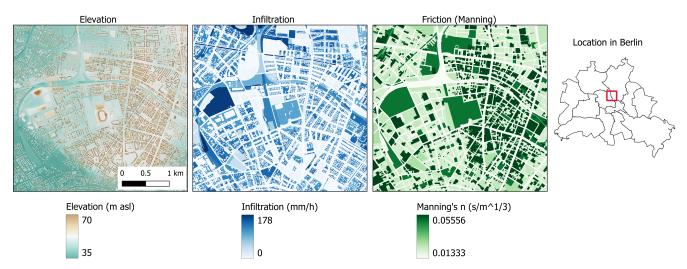
For the surface flow model, spatially distributed friction and infiltration values were generated based on soil data, land use, and sealing degrees. Manning's friction coefficients for the different land use types were selected from recommendations given



175



in Klimaatlas NRW (2024). Infiltration was considered with spatially distributed constant infiltration rates calculated based on the saturated hydraulic conductivity from the first 1 m of soil provided in the dataset Umweltatlas Berlin/Bodenkundliche Kennwerte 2015 multiplied with the unsealing degree calculated from sealing degrees of the unbuilt surfaces on a block area level provided in the dataset Umweltatlas Berlin/Versiegelung 2021. The average sealing degree of the unbuilt surfaces is about 26%. Buildings and roads were considered as completely sealed with an infiltration rate of zero, which is the case for 51% of the considered study area consisting of 35% roof and 16% road surfaces. The digital elevation model was modified to cut free the Gleimtunnel. Fig. 2 depicts the elevations including buildings, infiltration rates, and Manning's friction coefficients for the study area as well as its location within Berlin. The total simulation time was two hours, with precipitation occurring during the first hour, as only events with a 1-hour duration were selected for the hydrodynamic simulations, focusing on short, intense events.



Data sources: DGM: Geoportal Berlin/ATKIS ® DGM and Geoportal Berlin/ALKIS Gebäude; Infiltration based on Umweltatlas Berlin/Versiegelung 2021 and Umweltatlas Berlin/Bodenkundliche Kennwerte 2015; Land-use use from Geoportal Berlin/ALKIS Nutzung Flächen with Manning values from Klimaatlas NRW (2024)

Figure 2. Characteristics of the study area: Digital elevation model including buildings (left), infiltration rates (middle), and Manning's friction coefficients (right); the basic data used to create these maps are licensed under dl-de/by-2-0 (www.govdata.de/dl-de/by-2-0)

4 Results

180 4.1 Return levels

The relationship between intensity and duration for different event probabilities in the historical period of the climate simulation can be seen in Fig. 3. Due to the temporal resolution of the input data, the d-GEV could only be fitted using accumulation periods ≥ 1 hour (i.e. the region right of the vertical grey lines).



190

195

200

205



Heavy rain hazard maps are often based on an hourly 100-year event. For this probability and duration, Fig. 3 shows the return level from KOSTRA-DWD. The area-average of all cells located within the city limits of Berlin is denoted by a black cross, while the range of return levels from the individual cells is illustrated by the black horizontal line. The return levels from the historical simulation period match the station based KOSTRA-DWD values perfectly. For hydrodynamic modeling, an assumption must also be made about the temporal distribution of the hourly precipitation sum. A typically rainfall distribution used for design purposes and to generate pluvial flood maps is the so-called Euler-2 design rainfall (see Fig. 5). To construct an Euler-2 precipitation time series, sub-hourly intensities down to 5 minutes need to be known. These durations are not resolved by the model simulation but can be extrapolated using Eq. 1. As the comparison with KOSTRA-DWD for the 5-minute duration (0.08 h) shows, this approach is problematic. In comparison to KOSTRA-DWD, the extrapolated sub-hourly intensities are overestimated. The reason for this is that due to the missing sub-hourly data the parameter Θ describing the curvature of the IDF curves for sub-hourly durations, cannot be realistically fitted. The approach to overcome this problem is described in Sect. 4.3.

4.2 Climate change signal

A comparison between the three periods simulated with CCLM-CPS shows a clear increase in temperature with increasing GHG forcing for the study area (Fig. 4). In comparison with the mean temperature at the Berlin Dahlem station, the driving global model MIROC5 exhibits a positive bias, while the convection permitting model CCLM-CPS is around one Kelvin too cold during the reference period. The temperature trend in the scenario period is stronger in the global model than in the convection permitting model. In both models, the temperature variability beyond the trend decreases with increasing GHG concentrations.

The median of the hourly annual maximum rainfall intensities increases with increasing GHG concentrations (Fig. 1). The interannual variability is high and the events with the highest intensities occurred during the near future simulation period (simulation years 2045, 2051, 2059, and 2039). This is reflected in the statistical rainfall sums for probabilities associated with return periods beyond the length of the available data set (0.98 and 0.99), determined using the relationship described in 1. They increase compared to the historical reference period, but show a slight decrease when comparing the near future (2031-2060) to the far future (2071-2100; Fig. 3b). The difference between the two scenario periods is, however, within the confidence intervals of the IDF fit.

In terms of percent the increase of the 1-hour, 100-year return level compared to the historical period is +46% and +42% for the periods 2031-2060 and 2071-2100, respectively.





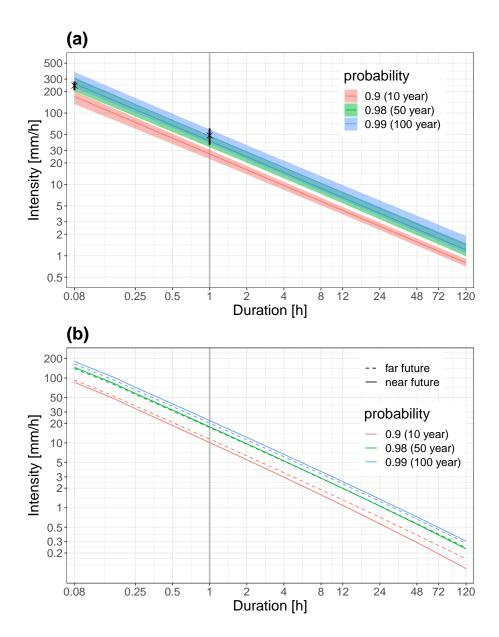


Figure 3. (a) Intensity-Duration-Frequency curves for the historical simulation. The colors distinguish 3 different non-exceedance probabilities (return periods). Shading denotes the 95% confidence interval. Black crosses mark the area-average values from KOSTRA for the 100-year return period. Black lines show the spread of the KOSTRA values for the 100-year return period over all Berlin grid cells. (b) Change in intensity between the historical period and the scenario period 2031-2060. The vertical grey line in (a) and (b) marks the temporal resolution of the model data (1-hour). Values for durations shorter than 1 hour are extrapolated. Please note the different scales.





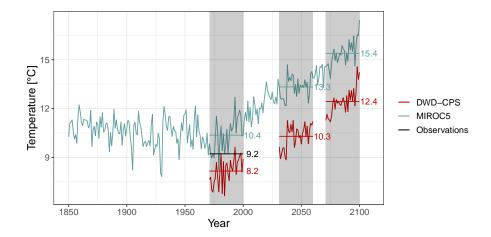


Figure 4. Temporal evolution of 2-m temperatures. Blue shows the time series of the driving model MIROC5 for the gridbox closest to central Berlin. Red is the time series for the 3 periods simulated with CCLM-CPS (mean over all grid boxes located within Berlin). As a reference the time mean for the period 1971-2000 from observation station Berlin is included in black. The grey rectangles mark the 30-year periods downscaled with CCLM-CPS.

4.3 Flooding

220

The following heavy rain events have been simulated with the coupled 2D-1D hydrodynamic model to study their impact on urban flooding in the selected area of Berlin:

- Historical 100a: 1-hour 100-year event of the CCLM-CPS simulation period 1971-2000 with a rainfall sum of 47.7 mm/h (-2% compared to the KOSTRA 100a event)
 - Future 100a: 1-hour 100-year event of the CCLM-CPS simulation period 2031-2060 with a rainfall sum of 69.8 mm/h
 (+46% compared to the Historical 100a event)
 - Strongest: the strongest 1-hour event within the three 30-year periods of CCLM-CPS simulations with a rainfall sum of 106.7 mm/h (+123% compared to the Historical 100a event)

Since the 100-year events for the near and far future simulations were very similar and the near future event even a bit stronger, only the 100-year event of the near future period was chosen for the hydrodynamic simulations. For the construction of the Euler-2 design rainfall, intensities for duration classes of less than one hour are needed. As already explained in Sect. 4.1, the precipitation output from the used climate simulations is one hour and extrapolating sub-hourly intensities from the modelled probability distribution leads to strong overestimations of sub-hourly intensities compared to values from KOSTRA. To address this, the selected approach involves using the sub-hourly Euler-2 distribution from the 100-year event according to KOSTRA-DWD-2020. Each 5-minute intensity value is scaled by a change factor, calculated as the ratio between the simulated 1-hour rainfall sum of the respective event and the 1-hour rainfall sum of the 100-year event from KOSTRA-DWD-2020 (48.5 mm).



230

235



The resulting change factors are 0.98 (47.7/48.5) for the Historical 100a event, 1.44 (69.8/48.5) for the Future 100a event, and 2.20 (106.7/48.5) for the Strongest event. For the Strongest event, the maximum intensity calculated with this approach is almost 9 mm/min, which would mean 45 mm in 5 min (as the used time step size for the Euler-2 construction is 5 min). This is considered to be unrealistically high (the maximum 5-min rainfall measured at the station in Berlin-Dahlem during the period 1979 to 2023 was 12.3 mm), but the results from similar temporal rainfall distributions are easier to compare to each other. To have a further comparison, all selected events were also simulated with a constant rainfall intensity. The results can then also be compared concerning the influence of the temporal rainfall distribution. Fig. 5 shows the Euler-2 and constant rain events for the three aforementioned rainfall sums.

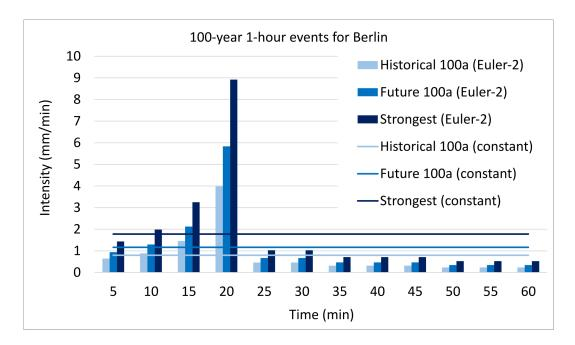


Figure 5. Rainfall inputs for hydrodynamic flood simulations with temporal distribution after Euler-2 design rainfall and constant rain intensities; Euler-2 intensities are constant over each 5-min interval

4.3.1 Climate change scenarios

Spatial distributions

Figure 6 shows the spatial distributions of simulated maximum water depths for the six simulated heavy rain events in the selected study area in Berlin. To enhance the visibility, not the whole, but a cropped extent of the model domain is depicted here. Water depths smaller 1 cm are set to transparent and are not depicted. The top row depicts the maximum water depths for the three selected events with a temporal rainfall distribution according to the Euler-2 design rainfall, and the bottom row for the events with a constant rainfall intensity. The Gleimtunnel, a known local flooding hotspot (Berliner-Zeitung, 2024), is illustrated in the detail. Flooding areas and water depths significantly increase between the Historical 100a, the Future 100a,





and the Strongest event as rainfall sums increase. The events with constant rainfall intensity generated smaller flooding areas and water depths than the Euler-2 rainfalls, which gets more pronounced with increasing rainfall sum. The flooding areas in the parks (visible through green color from the underlying OpenStreetMap) are much smaller in the case of constant than Euler-2 rainfall. This implies that during constant rainfall, less surface runoff is generated in the parks than during an Euler-2 rainfall, as the rainfall intensity not or rarely exceeds the infiltration rate of the soil. Even in the case of the Strongest event with constant intensity, there is almost no flooding in the parks.



Figure 6. Maximum water depths (m) for different rainfall sums (Historical 100a, Future 100a, and Strongest event) and temporal distributions (Euler-2 and constant) (values smaller 0.01 m are set to transparent and are not shown)

Fig. 7 depicts the surface runoff in terms of the unit discharge as product of water depth and flow velocity. According to Martínez-Gomariz et al. (2016), a value of $0.22 \text{ m}^2/\text{s}$ can be considered as threshold for the stability of pedestrians. In Fig. 7, orange to pink colors indicate surface runoff between 0.2 and $0.4 \text{ m}^2/\text{s}$, exceeding the stability threshold, while yellow indicates a surface runoff between 0.02 and $0.2 \text{ m}^2/\text{s}$, thus stable conditions for pedestrians.

It can be seen that the stability threshold is barely exceeded in the events with constant intensity. For the Euler-2 rainfalls, the Future 100a and the Strongest event lead to areas at the east entrance of the Gleimtunnel where the stability threshold is exceeded. Overall, the Euler-2 rainfalls lead to more surface runoff depicted by the yellow color on almost all roads, while the constant rainfalls show many more areas with surface runoff $\leq 0.02 \text{ m}^2/\text{s}$, which is set to transparent.

250

255



265





Figure 7. Maximum surface runoff (m²/s) for different rainfall sums (Historical 100a, Future 100a, and Strongest event) and temporal distributions (Euler-2 and constant) (values 0.02 m²/s are set to transparent and are not shown)

Temporal developments at the Gleimtunnel

To get a better understanding of the flood development over time and the differences between the different events at one specific flooding hotspot, Fig. 8 depicts the temporal developments of water depth (left) and surface runoff (right) as maximum values over one longitudinal section through the Gleimtunnel. For both temporal rainfall distributions, constant and Euler-2, the peak water depth significantly increases with increasing rainfall. The differences in the magnitude of peak water depth between constant and Euler-2 rainfall distributions are much larger for the Strongest event than for the Historical 100a and Future 100a events. The increase in peak water depth between the Historical and the Future 100a event is 51% for Euler-2 and 47% for constant rainfall, and between the Historical 100a and Strongest event 137% for Euler-2 and 109% for constant rainfall. The time to peak mainly depends on the rainfall distribution and not on the rainfall sum. The constant rainfalls generate peak water depths around half an hour later than the Euler-2 rainfalls. The temporal developments of surface runoff in the right panel of Fig. 8 show that the Strongest event leads to an earlier start and much higher magnitudes of surface runoff than the Historical 100a and Future 100a events, while in case of Euler-2 rainfalls, the main peak of the Strongest event occurs later than the ones of the Historical 100a and Future 100a events. The Historical 100a event with constant rainfall does not generate a pronounced peak runoff and shows overall relatively small surface runoff values of maximum 0.02 m²/s.





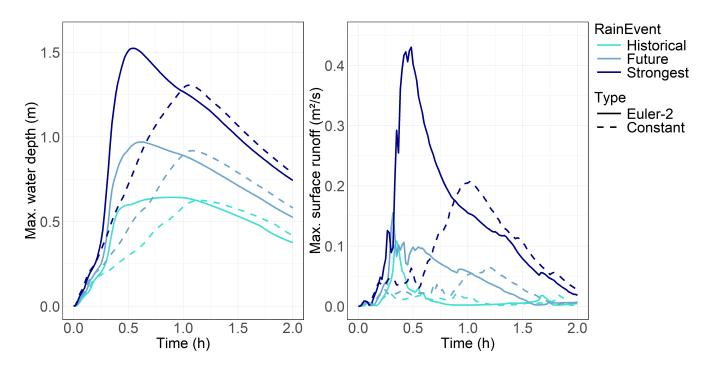


Figure 8. Temporal development of water depth (left) and surface runoff (right) for different rainfall events (maximum values along a longitudinal section through the Gleimtunnel)

As a coupled model of the flow on the surface and in the subsurface drainage system is used, the effects of different rainfall amounts and temporal developments in the drainage system can be assessed as well. Fig. 9 presents exemplarily the results of the outflow at one model outfall, which reflects combined sewer overflow (CSO) into the nearby river. For the simulated period, the CSO average flow rate and overall volume increase from the Historical 100a to the Future 100a event by 33% for Euler-2 rainfall and 27% for constant rainfall, and from the Historical 100a to the Strongest event by 74% for Euler-2 and 68% for constant rainfall. As depicted in Fig. 9, the flow has not stopped yet at the end of the simulation time, so the differences in the final overall volumes might be a bit different than the numbers given above. In the case of constant rainfall, CSO starts later and has later peaks, but with almost the same magnitudes. In the following, effects of infiltration, the drainage system, and the retention of rainwater from roofs are presented for different heavy rain events. For simplicity, only results with Euler-2 rainfalls are presented.

4.3.2 Effects of selected mitigation measures

285

The setup from the previous section - namely with consideration of infiltration and the subsurface drainage system, and without retention roofs - is considered as the reference case. This can be considered as current state of the considered study area, neglecting the few green roofs which already exist. In the following, three different setups are compared to the reference case for different rainfall events: 1) simulations without infiltration to indirectly estimate the negative impacts in case of further surface





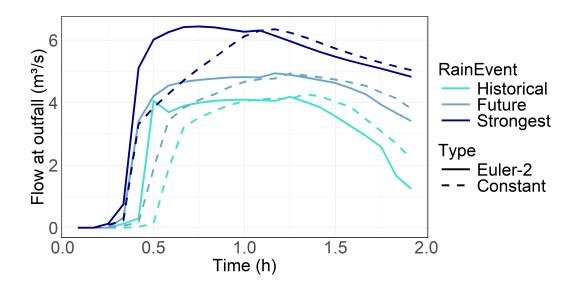


Figure 9. Temporal development of combined sewer overflow into the nearby river at one model outfall

sealing or on the other hand the effectiveness of large-scale surface desealing, 2) simulations without the drainage system to quantify the effectiveness of the actual subsurface grey infrastructure for extreme rainfalls under current and future climate, and 3) with all roof surfaces as retention roofs representing one example of blue-green infrastructure through the idealization that all roofs can capture the whole rainfall, even in the case of the Strongest event. These simulations are not intended to represent realistic scenarios, but rather to explore the range of possible system behaviors and assess the sensitivity of flooding dynamics to infiltration, drainage, and retention roofs.

Spatial distributions

300

305

Figure 10 depicts the spatial distributions of the differences in maximum water depths between the simulations without and with infiltration, drainage, and retention roofs, respectively. The left panels represent the Historical 100 event, and the right panels the Strongest event, both for Euler-2 rainfalls. Blue colors show the reductions while orange to red colors indicate increases due to the considered measure. The top panels illustrate the differences between the simulations without and with infiltration. Reductions between 1 and 10 cm occur in large parts of the model domain, while at flooding hotspots, such as the Gleimtunnel, reductions between 10 and 30 cm have been simulated. At a few locations, the simulation results show reductions of 30 cm and more.

The middle panels display the differences between the simulations without and with consideration of the drainage system. The results illustrate, that the drainage system effectively reduce flooding areas and water depths specifically at local hotspots, even in the case of the Strongest event. Nevertheless, high water depths still occur in large parts of the model domain as shown in the results for the reference case with drainage in Sect. 4.3.1. For the Historical 100a event as well as the Strongest event, reductions of more than 1 m in the area of the Gleimtunnel and between 0.5 and 1 m at another local flooding hotspot are



315

320

325

330

335



reached due to the drainage system. At several other roads, reductions between 0.1 and 0.5 m occur. The areas in orange to red color indicate overflow from the drainage system to the surface. This is simulated only at one location at railway tracks northwest of the Gleimtunnel. While this proofs the functioning of the bi-directional coupling of the surface and the drainage model, the plausibility of overflow at this location would need to be further checked, as it might be generated due to missing information on additional drainage infrastructure from the train company, which is not included in the used drainage model.

The bottom panels illustrate the spatial distribution of differences in maximum water depths for the simulations without and with full retention of rain on all roof surfaces. In large parts of the model domain, the retention roofs lead to reductions of up to 10 cm for both events. In some backyards, reductions of more than 40 cm are reached, but these details are not easily visible with the shown scale. Furthermore, the retention roofs lead to significant reductions of the flooded area in and around the Gleimtunnel, and the maximum water depths here are reduced by up to 30 cm in the Historical 100a event and up to 40 cm in the Strongest event. This example of flood reduction in case of full retention of the rain on all roof surfaces can be seen as a best-case scenario. While the complete retention during all considered heavy rain events could hardly be realized by modifying all roofs in the model domain to become green or retention roofs, it could - in theory - be achieved with combinations of green and/or retention roofs and cisterns for all buildings in that area. The stored water could also help conserve drinking water by being used for non-potable purposes, such as toilet flushing or irrigation.

Temporal developments at the Gleimtunnel

Figure 11 shows the temporal development of the maximum water depth (left) and surface runoff (right) in the Gleimtunnel for the different scenarios. In the top panel, the results with and without infiltration are depicted. The peak water depth of the Historical 100a and the Strongest event increased by 33% and 18% respectively, if infiltration is not considered. While the peak runoff of the Strongest event is increased, it is nearly the same for the Historical 100a event. The runoff volume is increased in both events.

The middle panels compare the results without and with consideration of the drainage system. On the left, the temporal developments of maximum water depths illustrate the effectiveness of the drainage system. In the case with drainage, the water depth decrease over time, while in the case without drainage, water depths are still rising until the end of the simulation time of two hours, while the rainfall stopped already after one hour. The maximum water depth until the end of the simulation time is 170% (Historical 100a), 154% (Future 100a), and 110% (Strongest event) higher without drainage compared to the simulations with drainage. Even though the effectiveness of the drainage system decreases with increasing rain intensity, its tremendous effect on flood reduction is still given for the Strongest event. The right middle panel shows the effects of drainage on the surface runoff. While for the Historical 100a and the Future 100a events, both peak and volume of surface runoff are higher without the drainage system, the hydrograph shape for the Strongest event appears differently, showing a much faster decline than in the case with drainage. This can be explained by the (earlier) generation of a larger and deeper flooding in and around the tunnel reducing the flow velocity inside the longitudinal section that was considered for the temporal developments in the Gleimtunnel.





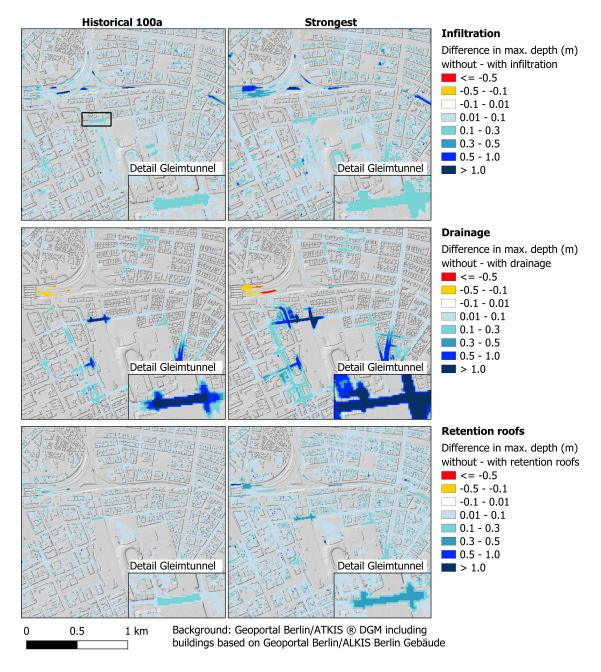


Figure 10. Spatial distributions of differences in maximum water depths for Euler-2 rainfalls between: without and with infiltration (top), without and with consideration of the drainage system (middle), and without and with full retention on all roofs (bottom); negative differences (orange to red colors) indicate increases in maximum water depth due to overflows from the drainage system to the surface

The bottom panels illustrate the effects of retention roofs on maximum water depths and surface runoff in the Gleimtunnel. The peak water depth is reduced by 22% (Historical 100a), 23% (Future 100a), and 24% (Strongest event), respectively,





showing very similar numbers and a small tendency to higher effectiveness with increasing rainfall intensity. Full retention was considered for all three events, but in the case of the Strongest event with 106.7 mm/h, it has to be pointed out that a full retention of more than 100 l/m² is less realistic than the full retention of about 50 or 70 l/m² as considered in the other two events. The temporal developments of surface runoff depicted on the right illustrate how much the surface runoff could be reduced through retention roofs, especially in the case of the Strongest event. While the simulation without retention results in a clear exceedance of the stability threshold of 0.22 m²/s after Martínez-Gomariz et al. (2016), the simulation with retention shows that the peak runoff could be reduced below the stability threshold. In the spatial distributions (which are not shown) it gets clear, that the threshold is still exceeded, but in a smaller area, which was not included in the longitudinal section considered for the extraction of temporal developments in the Gleimtunnel. Still, it emphasizes that the retention roofs in the surroundings not only reduce the water depths at local flooding hotpots but also dangerous flow conditions for pedestrian and possibly cars, which is not considered here in more detail. The retention roofs as well as infiltration reduced the combined sewer overflow volume by about 15-20% each.

4.3.3 Flood volumes

355

360

365

375

To compare the effects of rainfall sum and temporal distribution, infiltration, drainage, and retention roofs on the flooding in the entire model domain, the sum of maximum water depths in the model domain is calculated for each simulation, which is called flood volume in the following. It has to be emphasized that these values do not represent the actual flood volume at a given time but rather an aggregated value that allows comparing the domain-wide effects of different settings and measures on the maximum water depths through one single value. Neumann et al. (2024) compared different scenarios with blue-green infrastructure in a similar way, while they included only cells with maximum depths higher than 10 cm. Table 1 lists the values of flood volumes and relative differences for all simulations, including a few more simulations than the ones presented in the previous sections. First, the results of the simulations presented in the previous sections will be discussed, followed by the results of the additional simulations.

Effects from rainfall sum and temporal distribution, infiltration, drainage, and retention roofs

A first conclusion is that in the case of Euler-2 rainfall distributions, increases in the rainfall sum of 46% (Future 100a) and +123% (Strongest event), respectively, lead to increases in the flood volume of 61% (Future 100a) and 172% (Strongest event) compared to the Historical 100a event. The results show a non-proportional relation between rainfall sum and flood volume, with stronger increasing flood volume compared to the increase in the rainfall sum.

Comparing the flood volumes between Euler-2 and constant rainfall, constant rainfall leads to 48% (Historical 100a), 46% (Future 100a), and 39% (Strongest event) smaller flood volumes than the respective event with a temporal rainfall distribution according to the Euler-2 design rainfall. These significant differences emphasize the importance of the temporal rainfall distribution and the need for sub-hourly rainfall intensities, while there is a tendency to decreasing importance with increasing rainfall sum. The simulations without infiltration show an increase in flood volume of 75% (Historical 100a) and 40% (Strongest event), respectively. Thus, even in such densely urbanized area (51% is considered to be completely sealed by





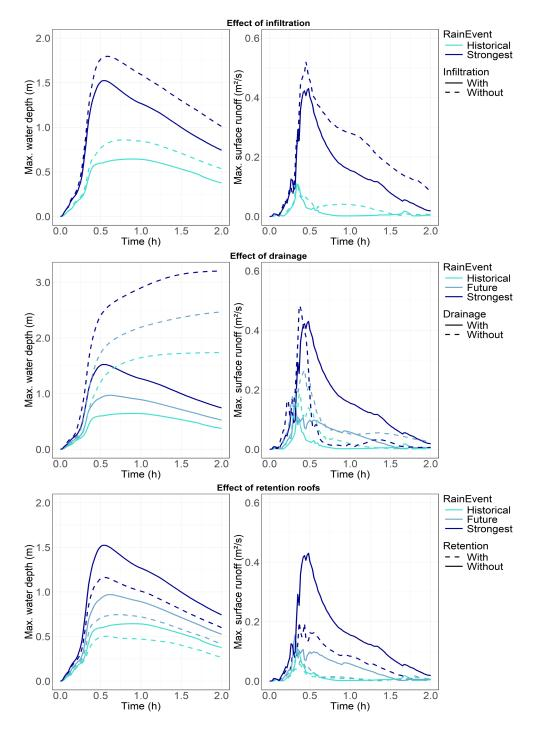


Figure 11. Temporal development of water depth and surface runoff within the Gleimtunnel without and with infiltration (top), the drainage system (middle), full retention roofs (top) - for Euler-2 rainfalls, maximum values along a longitudinal section through the Gleimtunnel; solid lines represent the reference case (with drainage and infiltration, without retention roofs)





buildings and roads, while the average sealing degree of unbuilt surfaces is around 26%), infiltration is strongly influencing the surface flooding, showing a decreasing importance with increasing rainfall sum. The combined effects of temporal rainfall distribution and infiltration, as well as time-dependent infiltration approaches could further be elaborated, but are beyond the scope of this study. The effect of the drainage system on the overall flood volume is reflected by reductions of 44% (Historical 100a), 39% (Future 100a), and 35% (Strongest event), respectively, showing a slightly decreasing effectiveness with increasing rainfall sum. As presented in the previous section, the drainage system is particularly successful in reducing the highest water depths at local hotspots. The retention roofs lead to reductions in flood volume of 37% (Historical and Future 100a) and 35% (Strongest event), respectively. As in the selected scenarios the retention roofs decreased the same percentage of the overall rain volume for all events, their effect on the flood volume for the different events is almost the same. For the Historical 100a event, the influence on the flood volume can be ranked as follows: 1) Infiltration (75%), 2) Temporal rainfall distribution (48%),
390 3) Drainage (44%), and 4) Retention roofs (37%). For the Strongest event, the ranking is: 1) Infiltration (40%), 2) Temporal rainfall distribution (39%), and 3) Drainage and Retention roofs (both 35%).

Results from additional simulations

For the Historical 100a event, one simulation with a horizontal resolution of 2 m instead of 5 m was carried out. The overall flood volume increased by 2%, which can be considered as a relatively small effect of the finer model resolution. Also the temporal development of maximum water depth in the Gleimtunnel is almost the same (not shown here). The computation time increased by a factor of 3.3 from 2.4 hours (5 m resolution) to 7.8 hours (2 m resolution) while using 48 CPU cores (Intel Cascade Lake Platinum 9242) for both simulations. Furthermore, one simulation without infiltration and drainage system was carried out, showing a 14% higher flood volume increase than if the increases of the simulations without either infiltration or drainage system are summed up (133% compared to 44% + 75% = 119%). This reflects the interaction of both processes infiltration and drainage through the underground pipe system. Further additional simulations for all three heavy rain events were carried out without the underground Mauerpark storage, which was completed in 2020 and provides an additional storage volume of 7500 m³ in the drainage system. Comparing the simulation results without the Mauerpark storage to the reference simulations with Mauerpark storage showed a difference of 2% in the overall flood volume for all three rainfall events. The spatial distributions of maximum water depths (not shown here) revealed that Mauerpark primarily reduced water depths near the Gleimtunnel, close to the storage location. Additionally, it decreased surface overflow from the drainage system at locations farther away. For the Historical 100a and the Future 100a events, the percentage reductions in maximum water depth in the Gleimtunnel are 16% and 9%, respectively, and in the combined sewer overflow volume 3% and 1%, respectively, indicating a decreasing effect with increasing rainfall intensity.

0 4.4 Discussion

395

400

405

In this study the effect of climate change on extreme precipitation probability is studied and the resulting urban flooding is quantified. For our study region Berlin only one global and regional climate model combination (MIROC5-CCLM) with convection permitting resolution was available at the time of the study. The analysis is based on the three available 30-year



415

420

425

430



Table 1. Flood volumes and relative differences

	Historical	Future	Strongest	Historical	Future	Strongest
Case	Flood volume (x 1000 m ³)			Relative difference to Historical Euler-2		
Euler-2	121	195	328	-	+61%	+172%
					Relative differences to respective Euler-2	
Constant	63	105	200	-48%	-46%	-39%
With Retention Roofs	76	123	213	-37%	-37%	-35%
Without Drainage	174	271	442	+44%	+39%	+35%
Without Infiltration	212	-	458	+75%	-	+40%
Cellsize 2 m	123	-	-	+2%	-	-
Without Infiltration and Drainage	281	-	-	+133%	-	-
Without Mauerpark storage	124	199	333	+2%	+2%	+2%

simulation periods forced with observed GHG concentrations (1971-2000) and RCP8.5 conditions for the periods 2031-2060 and 2071-2100. For Berlin the simulations show an increase in extreme precipitation frequency and intensity during the climate scenario periods compared to the historical period for short duration events that are relevant for pluvial flooding. Such an increase is also reported by other studies analyzing other regions in Germany with different regional model simulations at comparable resolution (Meredith et al., 2019; Hundhausen et al., 2024). While the median of the annual maximum hourly precipitation events in the MIROC5-CCLM simulations increases with increasing greenhouse gas concentrations, the most extreme events over Berlin are simulated during the near future rather than the far future period. As a consequence, the hourly return levels for the 100-year event, which we use as input for the hydrodynamic simulations, are highest during the near future period. This is unexpected as other studies suggest a steady increase of extreme precipitation probability which is most pronounced for high return periods and short durations (e.g. shown for Southern Germany in Hundhausen et al., 2024). To obtain more robust results an ensemble of climate scenario simulations is required. In order to address the uncertainties associated with the climate scenario, the ensemble should comprise simulations forced with different greenhouse gas concentration pathways. Such an ensemble is currently produced under the NUKLEUS project framework and should be soon available for future studies (BMBF, 2024).

To quantify the effects of changes in heavy rainfall on urban flooding, hydrodynamic simulations are needed, preferably by coupling flow processes on the surface and in the drainage system. Due to a lack of data such simulations usually include some simplifications and assumptions. In this study, flow processes on the surface and in the subsurface drainage system have been bi-directionally coupled. As shown in the results, infiltration had a significant effect on the flooding, even though the study area is highly urbanized, emphasizing the importance of urban green areas and possible desealing of currently sealed surfaces. But the spatial extent of such measures would need to be large to have significant effects. As soil and surface parameters might be very heterogeneous - especially in urban areas - which is still difficult to capture, the estimation of infiltration comes along with



450

455

460

465



a large uncertainty and the results have to be taken with care. Another simplification is that the direct drainage from roofs into the drainage system was neglected assuming that during the considered short and very intense events, most parts of the rainfall cannot be directly drained into the drainage system but will instead flow over the emergency overflows from the roofs to the traffic space or backyards. Furthermore, local details such as culverts or building passages were not specifically considered in this study.

In the current study, retention roofs are modeled using a simplified approach. In contrast, Neumann et al. (2024) applied Low Impact Development (LID) elements in the Storm Water Management Model (SWMM) within a 2D/1D surface runoff model for a different study area also in Berlin. In their study, the roof areas are not modeled as 2D surfaces, but as subcatchments connected to the nearest manhole. Additionally, retention roofs are defined in greater detail, using a list of parameters and multiple layers. Their findings demonstrated that retention roofs could fully retain rainfall from a 1-hour event with an intensity of 100 mm/h. Therefore, our simplified assumption of full retention is consistent with their results, even for the Strongest event of 106.7 mm/h.

Comparing the effects of infiltration, drainage system, retention roofs, and the additional storage below the Mauerpark on the maximum water depth in the local flooding hotspot Gleimtunnel gives the following ranking for the Historical 100a event: 1) Drainage (170%), 2) Infiltration (33%), 3) Retention roofs (22%), and 4) Mauerpark storage (16%). The effects on the overall flood volume are ranked differently: 1) Infiltration (75%), 2) Drainage (44%), 3) Retention roofs (37%), and 4) Mauerpark storage (2%). The drainage system is particularly efficient in reducing flooding at hotspots, the Mauerpark storage contributes to some extent to mitigating flooding specifically at Gleimtunnel, and the presented scenarios of infiltration and retention roofs across the entire catchment have distributed effects, while if realized in large spatial extent as in the given scenarios, they also contribute significantly to reductions at local hotspots. All effects decrease with increasing rainfall amount, except for the retention roofs, which by definition were able to retain the total rainfall for each of the three events in this study.

In Germany and several other European countries urban sewage systems are designed based on design rainfalls of Euler-2 type, where the type describes the temporal evolution of the event (hyetograph). Maps for pluvial flood risk in Berlin are based on Euler-2 type statistical 100-year hourly events. Two different types of design rainfalls (Euler-2 and constant) are compared in this study. The temporal evolution of the event influences the impacts. This has also been reported by Paton et al. (2024). While Paton et al. (2024) found that in Germany the severity of observed short extreme rainstorms often exceed the severity of the Euler-2 design rainfall events, for Poland Wartalska et al. (2020) found that Euler-2 design rainfalls have the tendency to be significantly larger than historic events. Both studies indicate that it would be desirable to use more realistic hyetographs than design rainfalls for the construction of risk maps.

Future work might encompass to assess further mitigation strategies. We found that replacing all customary roofs with retention roof is not sufficient to fully compensate the effect of climate change under the investigated scenario. Additional or alternative methods could be the inclusion of retention measures in the traffic space and desealing measures. Overall, multi-functional solutions combining several purposes are to be targeted. The sensitivity analysis explored the importance of infiltration on the impacts. Realistic scenarios of blue-green infrastructure and surface desealing could be elaborated in further modeling studies.





In this study, we focus on the Gleimtunnel, as it has a long history of flooding. However, the tunnel is of minor importance for Berlin's traffic network, and flooding there primarily causes local traffic disruptions and economic damages to car owners. Future studies could focus on flooding hotspots with high vulnerability, such as areas with critical infrastructure, schools, kindergartens, or social facilities located in low-lying areas.

5 Conclusions

485

490

495

Under climate change conditions the frequency and intensity of extreme precipitation events is expected to increase. The climate scenario simulations analyzed in this study for Berlin, Germany, predict a 46% increase in the intensity of a statistical 1-hour 100-year event in Berlin under RCP8.5 climate scenario conditions until the year 2060. In the Gleimtunnel, a notorious flooding hotspot, this leads to an increase in maximum flood height of 51% and peak surface runoff of 43%. The combined sewer overflow at one outfall of the drainage model increases by 33%.

The study is associated with a number of uncertainties. For the extreme rainfall analysis these include the choice of the climate scenario and the fact that only one global-regional model combination was available for the study. The hydrodynamic simulations are limited by uncertain infiltration settings and neglecting local details.

In this study we were able to demonstrate how hydrodynamic simulations can help to compare the effectiveness of different mitigation measures within an urban drainage catchment. A combination of measures will probably be needed to compensate for the effect of climate change. The plans of the Senate of Berlin to foster a transformation of the city into a "sponge city" by strengthening the role of green and blue infrastructure is a step towards a mitigation of the adverse effects but a more systematic and faster implementation is required.

Irrespective of the various uncertainties associated with this analysis, the investigation shows very clearly that urban flood risk maps must take climate change into account in order to adequately contribute to the protection of the population. Risk maps based on past observations with the assumption of a stationary climate will be soon outdated.

Code and data availability. Station data for Berlin data is available from the open data server of the DWD: https://opendata.dwd.de/climate_environment/CDC/observations_germany/climate/hourly/precipitation/historical/. The climate simulations are available from https://esgf. dwd.de/projects/dwd-cps (Haller et al., 2022a, b). KOSTRA design rainfalls can be downloaded from https://opendata.dwd.de/climate_environment/CDC/grids_germany/return_periods/precipitation/KOSTRA/. Surface data for Berlin is available from Geoportal Berlin under dl-de/by-2-0 licence (www.govdata.de/dl-de/by-2-0). The code for hms⁺⁺ is available on github (https://git.tu-berlin.de/wahyd/hmspp/hms

Author contributions. FT: conceptualisation, methodology, formal analysis, investigation, data curation, writing (original draft as well as review and editing), visualisation. KMN: conceptualisation, methodology, formal analysis, investigation, data curation, writing (original draft as well as review and editing), visualisation. LS: methodology, software, review. YZ: methodology, software, review. UU: supervision, review, project administration, funding acquisition. RH: supervision, review, project administration, funding acquisition.



505



500 Competing interests. U. Ulbrich is an editor for NHESS and K. Nissen a guest editor

Acknowledgements. Funding was received through the Einstein Research Unit 'Climate and Water under Change' from the Einstein Foundation Berlin and Berlin University Alliance, Grant number ERU-2020-609. This work used resources of the Deutsches Klimarechenzentrum (DKRZ) granted by its Scientific Steering Committee (WLA) under project ID 1229. The authors gratefully acknowledge the computing time made available to them on the high-performance computer "Lise" at the NHR Center NHR@ZIB. This center is jointly supported by the Federal Ministry of Education and Research and the state governments participating in the NHR (www.nhr-verein.de/unsere-partner). We would like to acknowledge Berliner Wasserbetriebe for providing their drainage model. The AI language model ChatGPT and the AI-powered writing assistant Grammarly were used to assist with text optimization and refinement in parts of this manuscript.





References

- Apel, H., Benisch, J., Helm, B., Vorogushyn, S., and Merz, B.: Fast urban inundation simulation with RIM2D for flood risk assessment and forecasting, Frontiers in Water, 6, https://doi.org/10.3389/frwa.2024.1310182, 2024.
 - Berliner-Zeitung: How will climate change impact Berlin?, https://www.berliner-zeitung.de/en/how-will-climate-change-impact-berlin-li. 172154, last access: 13. 9. 2024, 2024.
 - BKG: Land Nordrhein-Westfalen, Hinweiskarte Starkregengefahren, https://geoportal.de/Info/tk_04-starkregengefahrenhinweise-nrw, last access: 29. 1. 2025, 2021.
- BKG: Erfolgreicher Auftakt: Bundesweite Kartierung über die Gefahren durch Starkregen gestartet, https://www.bkg.bund.de/SharedDocs/ Pressemitteilungen/BKG/DE/PM_2023/230511-Kickoff-Starkregen.html, last access: 29. 1. 2025, 2023.
 - BMBF: NUKLEUS Nutzbare Lokale Klimainformationen für Deutschland, https://www.fona.de/de/massnahmen/foerdermassnahmen/RegIKlim/nukleus.php, last acess 17. 9. 2024, 2024.
- DWA: Deutsche Vereinigung für Wasserwirtschaft, Abwasser und Abfall: Arbeitsblatt DWA-A 118 Hydraulische Bemessung und Nachweis von Entwässerungssystemen, DWA-Bundesgeschäftsstelle, Berlin, Germnay, 2006.
 - EUR-Lex: DIRECTIVE 2007/60/EC OF THE EUROPEAN PARLIAMENT AND OF THE COUNCIL, 2007.
 - Fauer, F. S., Ulrich, J., Jurado, O. E., and Rust, H. W.: Flexible and consistent quantile estimation for intensity–duration–frequency curves, Hydrology and Earth System Sciences, 25, 6479–6494, https://doi.org/10.5194/hess-25-6479-2021, 2021.
 - Geoportal Berlin: https://www.berlin.de/sen/sbw/stadtdaten/geoportal/, last acess 11. 9. 2024.
- Haller, M., Brienen, S., Brauch, J., and Früh, B.: Historical simulation with COSMO-CLM5-0-16 version V2022.01 Downscaling of MIROC-MIROC5 data for Germany with 3 km grid spacing, https://doi.org/10.5676/DWD/CPS_HIST_V2022.01, 2022a.
 - Haller, M., Brienen, S., Brauch, J., and Früh, B.: Projection simulation with COSMO-CLM5-0-16 version V2022.01 Downscaling of MIROC-MIROC5 data for Germany with 3 km grid spacing, https://doi.org/10.5676/DWD/CPS_SCEN_V2022.01, 2022b.
- Hundhausen, M., Feldmann, H., Kohlhepp, R., and Pinto, J. G.: Climate change signals of extreme precipitation return levels for Germany in
 a transient convection-permitting simulation ensemble, International Journal of Climatology, 44, 1454 1471, https://api.semanticscholar.org/CorpusID:270475096, 2024.
 - IPCC: Impacts of 1.5°C Global Warming on Natural and Human Systems, p. 175–312, Cambridge University Press, https://doi.org/10.1017/9781009157940.005, 2022.
- Junghänel, T., Bär, F., Deutschländer, T., Haberlandt, U., Otte, I., Shehu, B., Stockel, H., Stricker, K., Thiele, L., and Willems, W.: Method-ische Untersuchungen zur Novellierung der Starkregenstatistik für Deutschland (MUNSTAR). Synthesebericht, https://www.dwd.de/DE/leistungen/kostra_dwd_rasterwerte/download/Synthesebericht_MUNSTAR_pdf.pdf, 2022.
 - Klimaatlas NRW: Methodik Papier zum Handlungsfeld Überflutungsschutz: Starkregengefahrenhinweiskarte des BKG für NRW, https: //www.klimaatlas.nrw.de/sites/default/files/2024-01/Methodik_Papier%20Starkregengefahrenhinweiskarte.pdf, last acess 11. 9. 2024, 2024.
- KOSTRA: Koordinierte Starkniederschlagsregionalisierung und -auswertung des DWD, https://opendata.dwd.de/climate_environment/CDC/grids_germany/return_periods/precipitation/KOSTRA/KOSTRA_DWD_2020/, last acess 11. 9. 2024, 2020.
 - Koutsoyiannis, D., Kozonis, D., and Manetas, A.: A mathematical framework for studying rainfall intensity-duration-frequency relationships, Journal of Hydrology, 206, 118–135, https://doi.org/https://doi.org/10.1016/S0022-1694(98)00097-3, 1998.



570



- Li, Y., Wang, P., Lou, Y., Chen, C., Shen, C., and Hu, T.: Assessing urban drainage pressure and impacts of future climate change based on shared socioeconomic pathways, Journal of Hydrology: Regional Studies, 53, 101760, https://doi.org/https://doi.org/10.1016/j.ejrh.2024.101760, 2024.
 - Lucas-Picher, P., Argüeso, D., Brisson, E., Tramblay, Y., Berg, P., Lemonsu, A., Kotlarski, S., and Caillaud, C.: Convection-permitting modeling with regional climate models: Latest developments and next steps, WIREs Climate Change, 12, e731, https://doi.org/10.1002/wcc.731, 2021.
- Martínez-Gomariz, E., Gómez, M., and Russo, B.: Experimental study of the stability of pedestrians exposed to urban pluvial flooding, Nat Hazards, 82, 1259–1278, https://doi.org/10.1007/s11069-016-2242-z, 2016.
 - Meredith, E. P., Ulbrich, U., and Rust, H. W.: The Diurnal Nature of Future Extreme Precipitation Intensification, Geophysical Research Letters, 46, 7680–7689, https://doi.org/10.1029/2019GL082385, 2019.
- Neumann, J., Scheid, C., and Dittmer, U.: Potential of Decentral Nature-Based Solutions for Mitigation of Pluvial Floods in Urban Areas—A

 Simulation Study Based on 1D/2D Coupled Modeling, Water, 16, https://doi.org/10.3390/w16060811, 2024.
 - Paton, E., Tügel, F., Eckmann, L., Joseph, B., and Hinkelmann, R.: Compilation method of a catalogue of reasonable worst-case rainfall series for flash flood simulations of short, convective rainstorms, Journal of Hydrology, 635, 131091, https://doi.org/10.1016/j.jhydrol.2024.131091, 2024.
 - Rossman, L. and Huber, W.: Storm Water Management Model Reference Manual Volume I, Hydrology, Washington, DC, 2015.
- Rybka, H., Haller, M., Brienen, S., Brauch, J., Früh, B., Junghänel, T., Lengfeld, K., Walter, A., and Winterrath, T.: Convection-permitting climate simulations with COSMO-CLM for Germany: Analysis of present and future daily and sub-daily extreme precipitation, Meteorologische Zeitschrift, 32, 91–111, https://doi.org/10.1127/metz/2022/1147, 2023.
 - Simons, F.: A robust high-resolution hydrodynamic numerical model for surface water flow and transport processes within a flexible software framework, Ph.D. thesis, https://doi.org/10.14279/depositonce-9589, 2020.
- Steffen, L. and Hinkelmann, R.: hms++: Open-source shallow water flow model with focus on investigating computational performance, SoftwareX, 22, 101 397, https://doi.org/10.1016/j.softx.2023.101397, 2023.
 - Tügel, F., Kronke, E., Nissen, K. M., Gronau, P., Steffen, L., Ulbrich, U., and Hinkelmann, R.: Hydrodynamische N-A-Ensemblesimulationen mit variablen räumlich-zeitlichen Verteilungen von Starkniederschlägen, https://doi.org/10.14617/for.hydrol.wasbew.44.23, 2023.
 - Ulrich, J., Jurado, O. E., Peter, M., Scheibel, M., and Rust, H. W.: Estimating IDF Curves Consistently over Durations with Spatial Covariates, Water, 12, https://doi.org/10.3390/w12113119, 2020.
 - Umweltatlas Berlin: https://www.berlin.de/umweltatlas/, last acess 11. 9. 2024.
 - Wartalska, K., Kaźmierczak, B., Nowakowska, M., and Kotowski, A.: Analysis of Hyetographs for Drainage System Modeling, Water, 12, https://doi.org/10.3390/w12010149, 2020.
- Watanabe, S., Hajima, T., Sudo, K., Nagashima, T., Takemura, T., Okajima, H., Nozawa, T., Kawase, H., Abe, M., Yokohata, T., Ise, T.,

 Sato, H., Kato, E., Takata, K., Emori, S., and Kawamiya, M.: MIROC-ESM 2010: model description and basic results of CMIP5-20c3m experiments, Geoscientific Model Development, 4, 845–872, https://doi.org/10.5194/gmd-4-845-2011, 2011.
 - Zevenbergen, C., Fu, D., and Pathirana, A.: Transitioning to Sponge Cities: Challenges and Opportunities to Address Urban Water Problems in China, Water, 10, https://doi.org/10.3390/w10091230, 2018.